International Journal of Environmental Science and Technology (2019) 16:5707–5724
https://doi.org/10.1007/s13762-018-1951-0

ORIGINAL PAPER

Assessment of hexavalent chromium biosorption using biodiesel extracted seeds of *Jatropha* sp., *Ricinus* sp. and *Pongamia* sp.

S. Rangabhashiyam[1,3] · S. Sayantani[2] · P. Balasubramanian[1]

Received: 20 March 2017 / Revised: 21 July 2018 / Accepted: 3 August 2018 / Published online: 13 August 2018

Abstract

Biosorbents from the biomass of *Jatropha* sp. (JES), *Ricinus* sp. (RES) and *Pongamia* sp. (PES) biodiesel extracted seeds were used in natural form for the elimination of hexavalent chromium. The study performed by varying the parameters of biosorbents size, solution pH, biosorbents dosage, metal concentration, contact time and temperature. The equilibrium data were correlated with two parameter isotherm models. Biosorption isotherm modeling showed that the biosorption data better explained by the Langmuir isotherm model with maximum monolayer biosorption capacities of 28.57, 19.60 and 27.77 mg/g for JES, RES and PES, respectively. The applicability of pseudo-second-order kinetics was observed in all the three biosorbents. The results of thermodynamic analysis showed that the biosorption of Cr(VI) ions onto JES, RES and PES was spontaneous in nature. Cr(VI)-loaded biosorbents were evaluated for a recycle studies with 0.1 M NaOH solution. Experiments conducted using Cr(VI) solution along with the coexisting ions demonstrated that the presence of co-ions slightly reduced the biosorption capacities of the JES and RES. Results of current research demonstrated that the JES, RES and PES could be used for the elimination of hexavalent chromium from aqueous system.

Graphical Abstract

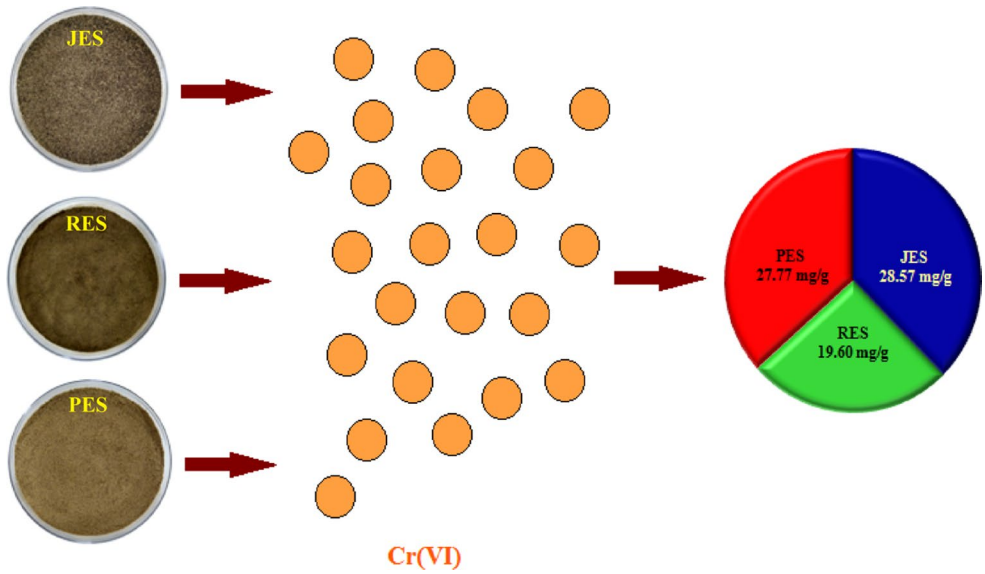

Keywords De-oiled biomass · Biosorption · Cr(VI) · Thermogravimetry · Isotherms

Editorial responsibility: M. Abbaspour.

Extended author information available on the last page of the article

Introduction

Water contamination with heavy metals is the major issue because of their toxicity effects, persistence nature and accumulation in the environment. Chromium is the 21st major copious element in the earth and with the aqueous solution concentration of about 122 mg/L (Hyder et al. 2015). Chromium exists in different oxidations states, out of which the Cr(III) and Cr(VI) are the more stable (Somdutta et al. 2012). The trace concentration of trivalent chromium participates in the sugar and fat metabolism of the living systems. Due to the limited hydroxide solubility property of trivalent chromium, it is less mobile and harmless. Hexavalent chromium is highly mobile, enters the soil and water bodies posing a tremendous risk to the environment. Since hexavalent chromium, a strong oxidizing agent gets easily adsorbed into the skin. The catastrophic health's effects of hexavalent chromium include cancer in the digestive tract, lungs as well in kidney, damage liver and gastric, respiratory diseases, nausea, diarrhea, nerve tissue damage, internal hemorrhage, skin irritation, nasal irritation, etc. (Umesh et al. 2009). The investigation of toxicity limits (LD_{50}) in the rat revealed 3250 mg Cr/kg for Cr(III) and 57 mg Cr/kg for Cr(VI). The United States Environmental Protection Agency had designated hexavalent chromium as priority toxic pollutants and set the acceptance limit value (Ying et al. 2014; EPA 1990). But the applications aspects of hexavalent chromium in the industrial sectors of electroplating, leather tanning, metal processing, artificial fertilizers, cement manufacture, wood preservation, textile dyeing, battery, paint and pigments, catalyst synthesis, etc., make it to consideration for utilization (Wen et al. 2015). Consequently, the elimination of hexavalent chromium containing effluent before discharge into environment allows proper utilization and prevents the harmful effects associated with it.

Different technologies include precipitation, coagulation-flocculation, flotation, oxidation, extraction, membrane separation, evaporation, etc., are existing. Nevertheless, the drawback of conventional technologies includes technically complex, requires more cost on initial investment, high operation and maintenance cost, non-selective, toxic sludge production, high energy and reagents requirements, lack of environmental friendly and unsuccessful removal at lower metal concentration (Mojdeh et al. 2009; Rangabhashiyam et al. 2018a). In order to bridge these gaps, an impending research is emphasizing on the biosorption technology. Biosorption refers to the physicochemical process subjects the biological material for the uptake of solutes. The process of biosorption involves the mechanisms of adsorption, absorption, ion exchange, precipitation, surface complexation and based on the affinity between the biosorbate and the biomass (Gadd 2009). The biosorption involves the biological material for the sequestration of contaminants in a passive manner, whereas the bioaccumulation is an active metabolic process. Biosorption is a potential bioremediation method gained noteworthy attention among the researchers working in the heavy metal removal. The biosorption process holds the merits of eco-friendliness, better selectivity, economical, free from secondary pollution generation, good recyclability of biomass, short processing time and no nutrient requirements (Rangabhashiyam et al. 2014a). Many developing countries suffer due to the water contamination with hexavalent chromium and the approach toward the costlier treatment methods may not be a feasible solution. Eliminating hexavalent chromium from industrial effluent is an important concern due to the issues of health hazardous effects and economic burdens associated with the contamination.

The seeds of *Jatropha* sp. (Svitlana et al. 2016), *Ricinus* sp. (Swaroopa et al. 2016) and *Pongamia* sp. (Radhakumari et al. 2016a) are used for production of biodiesel. The international *Jatropha* organization has stated that in the year of 2017; the worldwide cultivable lands 330,000 km^2 produce about 160 Mt of seeds. Out of which, Asia will be the major producer of *Jatropha* sp. seeds (Mohankumar et al. 2014). The average production of castor seed annually in India was 800,000 tonne, which accounts 75% of the world's production (Panwar et al. 2010). The Ministry of Agriculture, India, commenced the practice of plantation programs for *Pongamia* sp., since it acts as the valuable renewable feedstock source for the production of biodiesel and the annual yield of the *Pongamia* sp. seeds was about 200,000 tonne (Radhakumari et al. 2016b). After biodiesel extraction from seeds, a huge amount of waste biomass generated in the form of de-oiled cake, if left unprocessed which may cause negative impacts on the environment. The biomasses generated are eco-friendly, belong to renewable resources and suitable for the development of bio-related materials, which increases the economic profit (Jinjuta et al. 2016).

The current study involves the preparation of biosorbents from the biodiesel extracted seeds of *Jatropha* sp., *Ricinus* sp. and *Pongamia* sp., and their use in the biosorption of hexavalent chromium. Different process variables such as biosorbents size, solution pH, biosorbents dosage, concentration of metal ions and temperature were studied for the maximum hexavalent chromium biosorption. Various models of biosorption isotherms and kinetics were considered to analyze the metal removal process. Thermodynamic parameters were also found from the biosorption measurements. Biosorbents were checked for the recycle process by means of suitable desorbent concentration. In the binary system, the influence of salts and metal ions in the hexavalent chromium biosorption was also studied.

Materials and methods

Preparation of biosorbents

De-oiled biomass from the seeds of *Jatropha* sp., *Ricinus* sp. and *Pongamia* sp. was obtained separately from Energy Laboratory, Department of Mechanical Engineering of Periyar Maniammai University, India. The sample biomasses were subjected to distilled water wash to remove the dirt and soluble impurities associated with the biomass. The cleaned biomasses were oven dried at 60 °C for 48 h and further sieved to the different size ranges of 0.05–0.15, 0.15–0.2, 0.2–0.25, 0.25–0.3 and > 0.3 mm, respectively. The three prepared biosorbents from the biomass of *Jatropha* sp. (JES), *Ricinus* sp. (RES) and *Pongamia* sp. (PES), biodiesel extracted seeds were stored separately in airtight plastic container and used for further batch biosorption studies.

Preparation of Cr(VI) solution

The hexavalent chromium stock solution prepared using potassium dichromate and different concentration solutions of single-metal system of hexavalent chromium were obtained by dilution of the stock solution. The biosorption behavior of different coexisting ions was analyzed in binary system with 20 mg/L initial ion concentration. The chemicals employed in the present investigation were of analytical reagent grade and used without additional purification.

Characterization of the biosorbents

Elemental analyses of the biosorbents were measured with a ThermoScientific Flash 2000 elemental analyzer. The morphology of the biosorbents was observed with an environmental scanning electron microscopy (E-SEM) Quanta 250 FEG. Thermal stability of the biosorbents was checked through thermogravimetric analysis (TGA) in Shimadzu TGA 50 H instrument. X-ray diffraction (XRD) patterns of the biosorbents were recorded on Rigaku Ultima-IV. The functional groups of the biosorbent samples of native and Cr(VI) loaded were characterized qualitatively using PerkinElmer Spectrum Two.

Batch biosorption study

Experiments regarding the biosorption of hexavalent chromium by biomass of JES, RES and PES were performed separately in batch mode operation. The effect of experimental variables such as biosorbent size (0.05–0.15 to > 0.3 mm), biosorbent dosage (0.05–0.3 g), initial solution pH (2.0–8.0), initial metal ion concentration (20–100 mg/L), contact time (up to 120 min) and temperature (303–323 K) was studied. Stoppered conical flasks of 250 mL with the working volume of 50 mL known concentration of metal ion solution together with biosorbent were stirred at 120 rpm. Samples were collected at regular period, and the biomass was collected from the suspensions by means of filtration. The concentration of residual hexavalent chromium ions in the filtrate determined using diphenyl carbazide in the acidic solution. The equilibrium biosorption capacity of the biosorbent calculated according to the given equation:

$$q_e = \frac{(C_0 - C_e)}{m} \times V \quad (1)$$

where C_0, C_e represent the initial and the equilibrium Cr(VI) concentration (mg/L), m indicates the biosorbent dry weight (g) and V is the sample volume (L). The batch biosorption measurements were taken in duplicate to ensure reproducibility of the biosorption data.

The study over the influence of coexisting ions on the Cr(VI) biosorption was carried out in binary component removal system. Such study is essential, since the industrial effluents containing hexavalent chromium are associated with other ions. The binary component biosorption process involves the equal concentration of both hexavalent chromium and any one of the coexisting ions (Mg^{2+}, Ni^{2+}, Zn^{2+}, SO_4^{2-}, Cl^-). The experimental conditions include 50 mL solution containing both Cr(VI) and other foreign ions at 20 mg/L. After the sufficient contact time, the biosorbent was separated and filtrate was analyzed for the hexavalent chromium concentrations.

Desorption and regeneration experiments

To investigate the reusability of the JES, RES and PES, after the process of biosorption the experiments on desorption was performed by washing the metal loaded biosorbents with distilled water and then transferred into the desorbing solution containing 50 mL of 0.1 M NaOH. The biosorbents reconditioned for a subsequent biosorption process using distilled water. The Cr(VI) analysis in the solution conducted after a biosorption process performed using regenerated biosorbents.

Biosorption isotherms

The isotherm model describes the pollutants interaction with biosorbent materials; the mathematical correlations are significant in the optimization and modeling of biosorption process. Biosorption isotherms models constant values express the biosorbent surface properties and their affinities toward biosorbate. Many biosorption isotherm models have been successfully applied to biosorption experimental data (Rangabhashiyam et al. 2014b). In the present study,

isotherm models of Langmuir, Freundlich, Dubinin–Radushkevich, Halsey, Flory–Huggins, Temkin and Jovanovic were considered in the present study.

The Langmuir isotherm model

The Langmuir (1916) isotherm model is widely used in describing the saturation type of biosorption isotherms. According to this model, biosorption takes place at specific homogeneous and energetically identical biosorption sites on the biosorbent. The Langmuir equation in the nonlinear form is expressed as follows

$$q_e = \frac{Q_0 K_L C_e}{1 + K_L C_e} \tag{2}$$

where q_e is the biosorption capacity at equilibrium (mg/g), Q_0 is the maximum biosorption capacity (mg/g), C_e is Cr(VI) equilibrium concentration (mg/L) and K_L denotes the Langmuir isotherm constant (L/mg).

Equilibrium parameter (R_L) determined using the following expression:

$$R_L = \frac{1}{1 + K_L C_0} \tag{3}$$

The value of R_L represents the shape of the isotherm.

The Freundlich isotherm model

The Freundlich and Helle (1939) isotherm model describe the non-ideal and reversible biosorption process. This empirical model not restricted to the monolayer formation, based on the assumption of heterogeneous surface and non-uniform distribution of biosorption heat over the biosorbent surface without saturation of biosorption sites. The Freundlich equation is commonly presented as

$$q_e = K_f C_e^{1/n} \tag{4}$$

where K_f (mg/g) and n are the Freundlich coefficient related to biosorption capacity and biosorption intensity of the biosorbents. The Freundlich isotherm model constant $1/n$ also denotes the heterogeneity factor and values ranges between 0 and 1. The value of $1/n$ is close to 0 in case of the more heterogeneous surface.

The Dubinin–Radushkevich isotherm model

The Dubinin–Radushkevich (1947) isotherm model is more general isotherm than the Langmuir, since this model does not assume the concepts of homogeneous surface or constant biosorption potential. This model used to determine whether the nature of the biosorption processes carried out by means of physical or chemical mechanism. The Dubinin–Radushkevich equation can be written as follows

$$q_e = Q_m \exp^{K\varepsilon^2} \tag{5}$$

where Q_m is the maximum biosorption capacity (mg/g), K is the activity coefficient related to mean biosorption energy (mol^2/J^2), ε indicates the Polanyi potential and it is related to the equilibrium concentration, which is represented in the following equation

$$\varepsilon = RT \ln\left(1 + \frac{1}{C_e}\right) \tag{6}$$

where R denotes the universal gas constant (8.314 J/mol K), T represents the temperature (K). The mean biosorption energy E (kJ/mol) determined from the K value by using the expression of $E = 1/\sqrt{2K}$.

The Halsey isotherm model

The Halsey (1948) isotherm model is appropriate for the multilayer biosorption and demonstrates the heteroporous nature of the biosorbent. The model equation is as follows

$$q_e = \exp\left(\frac{\ln K_H - \ln C_e}{n_H}\right) \tag{7}$$

where K_H, n_H indicate the constant and exponent of Halsey isotherm model.

The Flory–Huggins isotherm model

The Flory–Huggins (Horsfall and Spiff 2005) isotherm model explains about the degree of surface coverage characteristics of biosorbate on biosorbent. The model has the following form

$$\frac{Q}{C_0} = K_{FH}(1 - Q)^{n_{FH}} \tag{8}$$

where Q represents the degree of surface coverage and related to the metal ion concentration by $Q = 1 - C_e/C_0$. K_{FH} is the Flory–Huggins isotherm constant and n_{FH} specify the model exponent.

The Temkin isotherm model

The Tempkin and Pyzhev (1940) isotherm model based on the assumption that due to the biosorbate–biosorbate repulsions the heat of biosorption of all the molecules in the layer decreases linearly with the molecules coverage and the biosorbate biosorption uniformly distributed. The model is expressed by the following relation

$$q_e = B_T \ln(A_T C_e) \tag{9}$$

where $B_T = (RT)/b_T$, b_T is the Temkin constant related to the heat of biosorption (kJ/mol), A_T represent the equilibrium binding constant (L/g), R is the universal gas constant (8.314 J/mol K) and T is the absolute temperature (K).

The Jovanovic isotherm model

The Jovanovic (1969) isotherm model considers of the possibility over mechanical contacts between the biosorbing and desorbing molecules. The Jovanovic isotherm corresponds to another estimate for monolayer localized biosorption without lateral interactions. The similar type of approximation directs to the result that monolayer biosorption of mobile hard disks is depicted by the Langmuir isotherm model. The Jovanovic equation may be written as:

$$q_e = q_{mj}\left(1 - e^{(K_j C_e)}\right) \tag{10}$$

where q_{mj} is Jovanovic isotherm model predicted maximum multilayer biosorption capacity (mg/g), K_j represent the Jovanovic constant (L/g).

Biosorption kinetics

Biosorption kinetics modeling is significant to understand the insight of metal biosorption onto biosorbents and to identify the rate-limiting step of the transport mechanism. The biosorption kinetics depends on the properties of biosorbent, biosorbate and the experimental conditions. The kinetics of metal removal by biosorbents has been widely tested using kinetic models. For the investigation over the biosorption mechanism and to determine the biosorbents performance toward Cr(VI) removal, the biosorption kinetic models such as pseudo-first-order, pseudo-second-order and intraparticle diffusion models were fitted with the experimental data.

Pseudo-first-order kinetic model

The pseudo-first-order kinetic model developed by Lagergren has the importance in the determination of the biosorption rate constant (Lagergren, 1898). In most of the metal biosorption studies, the pseudo-first-order kinetic model does not fit good to the complete contact time and normally pertinent only at the initial period of biosorption process. The linearized integral form of the pseudo-first-order kinetic model is shown as follows:

$$\log(q_e - q_t) = \log q_e - \frac{k_1}{2.303}t \tag{11}$$

where q_e and q_t are the amounts of metal ions biosorbed (mg/g) at equilibrium and at any time, t (min), respectively, and k_1 is the pseudo-first-order biosorption rate constant (1/min).

Pseudo-second-order kinetic model

The pseudo-second-order kinetic model (Ho and McKay 1999) predicts the metal removal behavior over the whole range of the process. The model considers the assumption that the rate-limiting factor may be because of chemisorptions involving valence forces by means of electrons sharing between the biosorbent functional groups and metal ions. The pseudo-second-order kinetic model can be applied in the following form

$$\frac{t}{q_t} = \frac{1}{k_2 q_e^2} + \frac{t}{q_e} \tag{12}$$

where k_2 (g/mg min) represent the rate constant of the pseudo-second-order kinetic model.

Intraparticle diffusion model

The biosorption of metal ions involves the different steps such as the metal ions movement onto biosorbent surface, diffusion to the interior pores refers to the intraparticle diffusion and interaction with binding sites on the biosorbent. The intraparticle diffusion model examines the possibility of intraparticle diffusion and assumed that the biosorbed amount is directly proportional to square root of the contact time (Weber and Morris 1962). In order to elucidate the diffusion mechanism, the experimental results were analyzed using the intraparticle diffusion model expressed as follows

$$q_t = k_{id} t^{1/2} + I \tag{13}$$

where k_{id} is the intraparticle diffusion model rate constant (mg/g $\text{min}^{1/2}$) and I is the intercept (mg/g).

Thermodynamic studies

The interactions between biosorbate–biosorbent and the resulting energy changes during biosorption process are elucidated through the thermodynamics parameter. The thermodynamic parameters including the Gibbs free energy ($\Delta G°$), enthalpy change ($\Delta H°$) and entropy change ($\Delta S°$) were used for the assessment over the thermodynamic feasibility and spontaneous nature of the metal removal process. The thermodynamics parameters obtained by using the below given expressions

$$\Delta G^{\circ} = -RT \ln K_C \tag{14}$$

$$\ln K_C = \frac{-\Delta H^{\circ}}{RT} + \frac{\Delta S^{\circ}}{R} \tag{15}$$

where Gibbs free energy ($\Delta G°$), enthalpy change ($\Delta H°$) and entropy change ($\Delta S°$) are the thermodynamic constants. K_c

is the distribution coefficient, which is related to equilibrium biosorption capacity and equilibrium metal ions concentration by $K_c = q_e/C_e$.

Results and discussion

Characterization of JES, RES and PES

The results of the physicochemical analysis (Namasivayam and Sangeetha 2006; Ayushi et al. 2017) of JES, RES and PES are given in Table 1. The environmental scanning electron microscopy (E-SEM) was carried out for the biosorbents of JES (Fig. 1a), RES (Fig. 1b) and PES (Fig. 1c) in order to evaluate their surface microstructures. The morphology of the biosorbents presents irregular rough surface, increased roughness, minor fissures and more compact fibrous material without any apparent porous structure, which is the characteristic feature of the biomaterials. The presence of such structures in the JES, RES and PES may contribute to the hexavalent chromium biosorption via the favorable environment for Cr(VI) ions retention between the interstices.

Table 1 Physicochemical analysis results of JES, RES and PES

Parameter	Value		
	JES	RES	PES
C	44.02	41.53	45.12
H	6.00	6.11	6.70
N	6.67	8.83	6.92
Surface area (m^2/g)	1.919	1.316	1.860
pH	6.62	6.04	5.74
pH_{ZPC}	7.29	7.62	7.74
Moisture content (%)	10.00	10.50	15.00
Ash content (%)	3.35	4.20	2.80
Volatile content (%)	54.45	52.75	59.65
Dry matter (%)	90.00	89.50	85.00
Fixed carbon (%)	32.20	32.55	22.55
Bulk density (g/cm^3)	1.25	0.83	1.00
Conductivity (mS/cm)	0.382	0.431	0.268

Thermogravimetric analysis (TGA) of JES, RES and PES samples revealed their thermal degradation characteristics. The thermogravimetric profiles of the biosorbents are presented in Fig. 2a. It can be seen from the thermogravimetric analysis graphs that decomposition of JES, RES and PES takes place in three distinct zones. The first zone of TGA profiles displays the moisture loss at around 100 °C (Oladoja et al. 2012). This may be attributed to the fact that at temperature higher than 100 °C the surface tension bound water of the biosorbents were lost, which resulted in the weight losses of 2.70%, 5.24% and 4.92%, for JES, RES and PES, respectively. The second zone with the temperature range of 150–450 °C, observed the weight losses of about 54.41%, 47.83% and 52.43% for JES, RES and PES biosorbents, respectively. The second zone of the thermogravimetric profiles can be referred to as the major zone of decomposition and this can be ascribed due to the decomposition of chemically bound water, cellulose, hemicelluloses and lignin in the biosorbents (Edidiong and Alastair 2016). Finally, the remaining highly non-volatile carbonaceous matters vaporize into CO and CO_2 at the temperature range of 450–720 °C (Rahulkumar et al. 2016) and JES, RES and PES contributed to weight losses of 25.35%, 24.80% and 35.43%, respectively. The third zone of thermogravimetric profiles indicated gradual weight losses by means of the slow decomposition of solid residue and resultant in the formation of char. The X-ray diffraction spectra of JES, RES and PES were analyzed at the scan range of 5°–110° and are illustrated in Fig. 2b. The diffraction patterns of the three biosorbents show amorphous broad hump and in the broadness of the peaks, and there observed some crystalline sharp peaks mounted on the broad pattern of each biosorbent spectra.

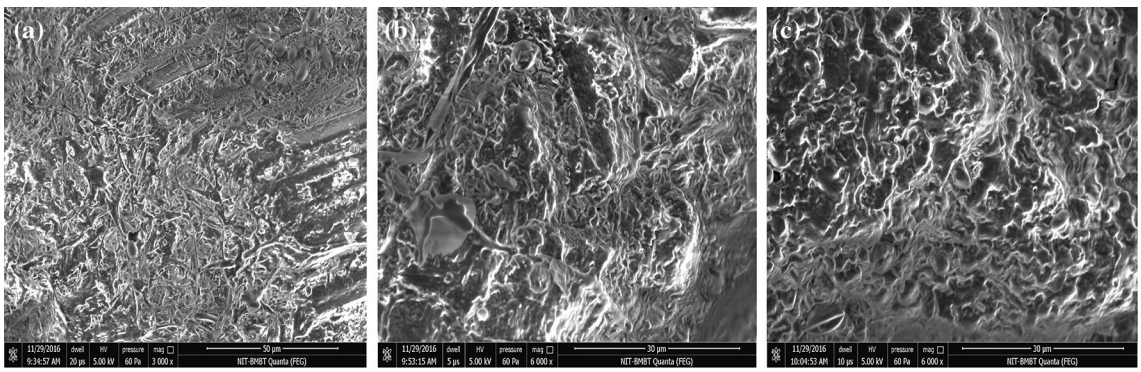

Fig. 1 The environmental scanning electron microscopy images of **a** JES, **b** RES and **c** PES

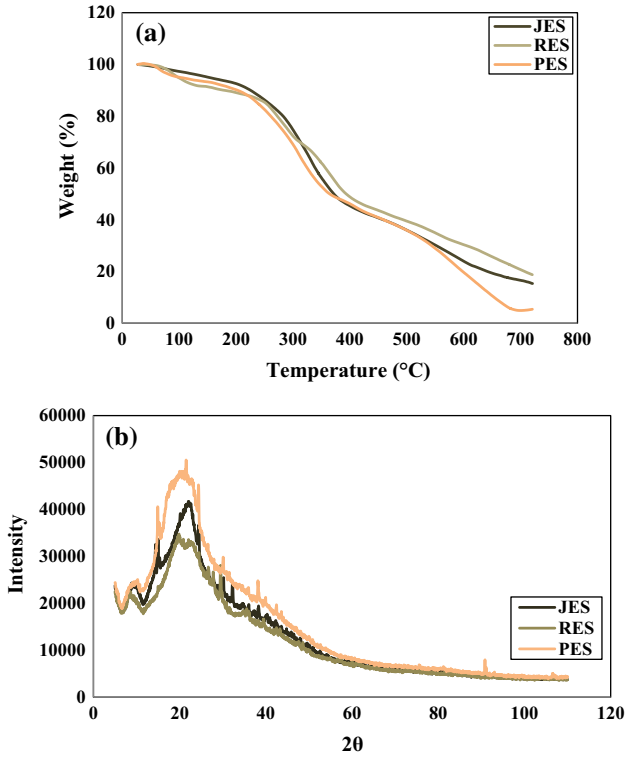

Fig. 2 Thermogravimetric analysis graphs (**a**) and X-ray diffraction patterns (**b**) of JES, RES and PES

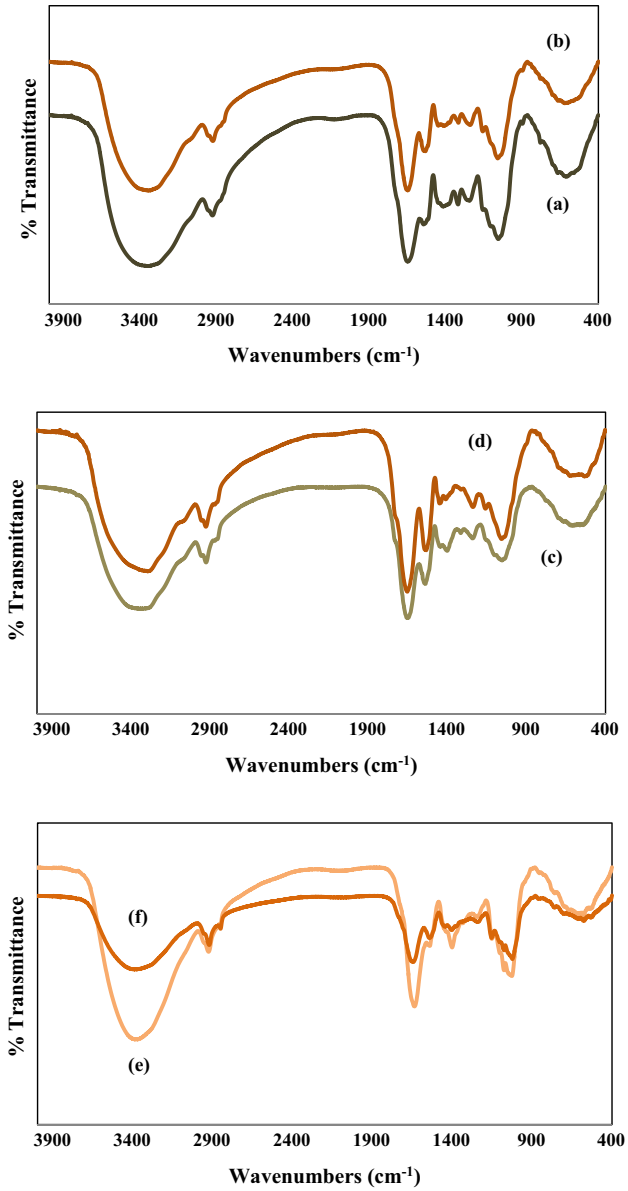

Fig. 3 FT-IR spectra of **a** JES, **b** Cr(VI)-loaded JES, **c** RES, **d** Cr(VI)-loaded RES, **e** PES and **f** Cr(VI)-loaded PES

FT-IR analysis provides valuable information regarding the presence of functional groups that take part in the process of biosorption. The vibration frequency changes in the functional groups of the biosorbents such as JES, RES and PES before and after hexavalent chromium biosorption were analyzed (Fig. 3) within the wave number range of 400–4000 cm^{-1}. The spectra of JES, RES and PES exhibit a number of vibrational bands representing the complex nature of the biomaterials. Table 2 represents spectral analysis of the biosorbents before and after Cr(VI) biosorption. The obvious shifts in the wave number were observed from 3356 cm^{-1} (JES) to 3347 cm^{-1} (Cr(VI)-loaded JES), 3346 cm^{-1} (CES) to 3299 cm^{-1} (Cr(VI)-loaded CES) and 3380 cm^{-1} (PES) to 3385 cm^{-1} (Cr(VI)-loaded PES). These shifts in the wave number represented that the biosorbents surface containing –OH group was one of the functional group involves with the binding of Cr(VI) ions. The stretching vibrations of the C–H groups and C=O stretching in carboxyl or amide groups were found as the minor peak shift in the Cr(VI)-loaded JES, CES and PES, respectively. In the presence of Cr(VI), a major peak shift took place from 1546 cm^{-1} (JES) to 1533 cm^{-1} (Cr(VI)-loaded JES) which indicates the N–H stretching of the primary amides, whereas CES and PES showed minor peak shift. The RES FT-IR spectrum showed intense bands around 1402 cm^{-1} which shifted to 1450 cm^{-1} for Cr(VI)-loaded RES. This was due to interaction of the COO– group in carboxylic acid with the Cr(VI) ions. A slight peak shift was observed in Cr(VI)-loaded JES, CES and PES in the function group region corresponds to the stretching vibration of C–OH of carboxylic acid. A minor band shift from 608 cm^{-1} (JES) to 620 cm^{-1} (Cr(VI)-loaded JES) and an intense bands shift from 602 cm^{-1} (CES) to 533 cm^{-1} Cr(VI)-loaded (CES) were attributed to the bending vibrations of aromatic compounds, which were involved in the biosorption

Table 2 FT-IR wave number and corresponding functional groups observed on JES, RES and PES for the biosorption of hexavalent chromium

JES	Cr(VI)-loaded JES	Differences	RES	Cr(VI)-loaded RES	Differences	PES	Cr(VI)-loaded PES	Differences	Functional groups
Band position (cm^{-1})									
3356	3347	9	3346	3299	47	3380	3385	− 5	OH stretching vibrations, –NH stretching
2929	2927	2	2929	2930	− 1	2928	2924	4	C–H stretching
1648	1648	x	1651	1654	− 3	1637	1646	− 9	C=O stretching in carboxyl or amide groups
1546	1533	13	1539	1535	4	1535	1541	− 6	N–H stretching of the primary amides
1419	1414	5	1402	1450	− 48	1402	1402	x	COO– group in carboxylic acid
1320	1317	3	x	x	x	x	x	x	O–H in-plane bending, C–N stretching
1246	1241	5	1241	1239	2	x	x	x	C–O stretch, $–SO_3$ stretching
1056	1061	− 5	1055	1058	− 3	1027	1024	3	Stretching vibration of C–OH group of carboxylic acid
608	620	− 12	602	533	69	581	573	8	Bending vibrations of aromatic compounds

of hexavalent chromium (Pehlivan et al. 2012; Gholamreza and Behnam 2010). There is also some other small shift of the bands noticed in JES, RES, PES, and their respective functional groups are O–H in-plane bending, C–N stretching, C–O stretch, $–SO_3$ stretching and stretching vibration of C–OH group of carboxylic acid. These functional groups in the biosorbents had shown trivial effect toward the removal of hexavalent chromium.

Effect of initial pH

The initial pH of the aqueous solution is one of the important factors that influence over the metal biosorption process. The biosorption capacity and removal efficiency of Cr(VI) using JES, RES and PES as a function of initial solution pH were investigated at 303 K and 20 mg/L initial Cr(VI) concentration. The biosorbents were observed effective toward Cr(VI) removal at an initial solution pH 2.0. It is obvious from the Fig. 4a, the removal of Cr(VI) decreases with an increase in initial solution pH from 2.0 to 8.0. The maximum removal of 9.94 mg/g (99.49%), 8.14 mg/g (81.40%) and 8.91 mg/g (89.15%) was found for JES, RES and PES, respectively. For all the biosorbents, the removal of Cr(VI) was affected dramatically by the further increase in initial pH from 2.0 to 8.0. In an aqueous system, the hexavalent chromium may exist in the ionic forms of $HCrO_4^-$, $Cr_2O_7^{2-}$ and CrO_4^{2-}. The stability of these ions in the aqueous solution mainly depends on the pH. The removal of Cr(VI) was higher in the lower pH ranges, because of the high electrostatic force of attraction. The presence of the more number of H^+ ions in the acidic pH range counterbalances the negative charge on the surface of biosorbent, resultant in an increased diffusion of chromate ions onto the biosorbents. At the higher initial pH solution, Cr(VI) biosorption was declined and the results are because of the presence of more number of OH^- ions that hinders the chromate ions diffusion (Anil et al. 2012).

The value of point of zero charge of JES, RES and PES was found as 7.29, 7.62 and 7.74, respectively. The surface of the biosorbents was positively charged at a pH value of less than point of zero charge. Consequently, anionic species could be biosorbed on the surface of JES, RES and PES. The biosorption of Cr(VI) species onto the biosorbents may be due to the direct exchange of ions with specific biosorbent surface functional groups. The initial pH of 2.0 was chosen for the experimental work toward the removal of dominating hexavalent chromium ion $HCrO_4^-$ from the aqueous solutions.

Effect of biosorbents size

The investigation over the effect of biosorbents size on the removal of Cr(VI) was performed by using initial Cr(VI) concentration 20 mg/L, 2.0 pH and by varying the biosorbents size of 0.05–0.15, 0.15–0.2, 0.2–0.25, 0.25–0.3 and > 0.3 mm. Figure 4b represents the biosorption capacity and percentage removal of Cr(VI) for the different particle sizes of JES, RES and PES, respectively. The removal of Cr(VI) decreased for JES, RES and PES, as the biosorbents size range increased from 0.05–0.15 to > 0.3 mm. The results reveal that smaller size of the biosorbent offers higher surface area with more number of binding sites and higher contact surfaces (Shalini et al. 2015). The highest biosorption capacity and percentage Cr(VI) removal of 9.97 mg/g (99.77%), 8.88 mg/g (88.82%) and 9.06 mg/g (90.67%) were observed for the JES, RES and PES size range of 0.05–0.15 mm. Therefore, smaller the biosorbent size has greater surface area resultant in higher removal of Cr(VI) from aqueous solutions.

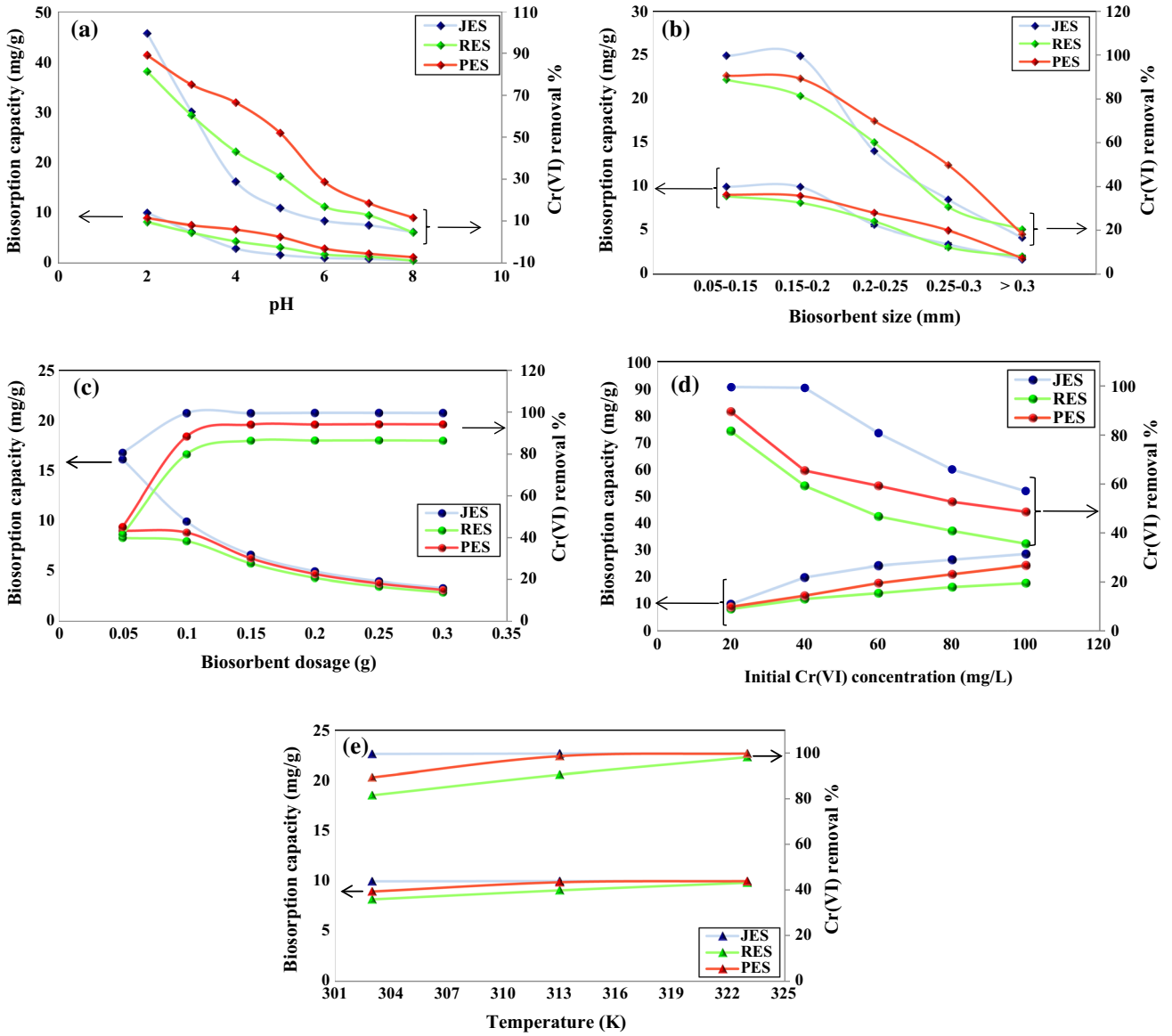

Fig. 4 Effect of **a** initial pH, **b** biosorbent size, **c** biosorbent dosage, **d** initial Cr(VI) concentration and **e** temperature on biosorption capacity and the percentage removal of Cr(VI) by JES, RES and PES

Effect of biosorbents dosage

The removal of Cr(VI) by JES, RES and PES was studied for the different biosorbents dosage of 0.05, 0.10, 0.15, 0.20, 0.25 and 0.3 g at initial Cr(VI) concentration of 20 mg/L and 2.0 pH. The effect of biosorbents dosage on the Cr(VI) removal process is shown in Fig. 4c. Biosorption capacity refers to the mass of Cr(VI) biosorbed per unit mass of biosorbent. As the biosorbent dosage increased from 0.05 to 0.3 g, the biosorption capacity of JES, RES and PES toward Cr(VI) removal showed a reduced effect from 16.13 to 3.32, 8.31 to 2.88 and 9.03 to 3.14 mg/g, respectively. This may be due to the fixed concentration of Cr(VI) was more shared by per unit mass of biosorbent with increased total biosorbent surface subsequent to the unsaturation of biosorption sites (Suresh and Babu 2009). Nevertheless, opposite trend was observed with the percentage removal of Cr(VI) by JES, RES and PES. For the biosorbents dosage above 0.15 g, the percentage removal of Cr(VI) for JES, RES and PES remained almost constant. This may be attributed to the equilibrium attainment between the biosorbent surface Cr(VI) concentration and the solution Cr(VI) concentration.

JES, RES and PES dosage of 0.1 g was chosen for the studies on the removal of Cr(VI) from aqueous solutions. This trend was in agreement with the earlier work of Cr(VI) removal using *Caryota urens* inflorescence waste biomass (Rangabhashiyam and Selvaraju 2015a, b).

Effect of initial Cr(VI) concentration

The effect of initial Cr(VI)concentration on biosorption capacity and percentage Cr(VI) removal is shown in Fig. 4d. For the studied initial Cr(VI) concentration range from 20 to 100 mg/L, the biosorption capacities of JES, RES and PES were found to increase from 9.96 to 28.51, 8.16 to 17.78 and 8.94 to 24.29 mg/g, respectively. The results may be due to equilibrium process of the biosorption system. Moreover, the higher Cr(VI) concentrations provide the significant driving force to overcome all mass transfer resistance between aqueous solution and biosorbent phase resulting in higher probability of collision between Cr(VI) ions and the biosorbents active sites. The results of the percentage removal of Cr(VI) by JES, RES and PES were observed reduced with respect to increase in the initial Cr(VI) concentration. This may be attributed to the competitive effect of more number of Cr(VI) for the available binding sites on the biosorbents, since the biosorbent dosage is kept constant. At low Cr(VI) concentration, the ratio of available biosorbent surface to the initial Cr(VI) concentration was larger and the removal efficiency of biosorbents was higher. But at higher Cr(VI) concentrations, this ratio was lower and resulted in the reduced percentage removal of Cr(VI) (Gannavarapu et al. 2012). Therefore, the removal of Cr(VI) by JES, RES and PES was dependent on the initial Cr(VI) concentration.

Effect of contact time

The contact time between the biosorbent and the biosorbate is a vital parameter, which is noteworthy for consideration in the industrial wastewater treatment. In order to determine the effect of contact time, the biosorption capacities of bisorbents toward different Cr(VI) concentration were evaluated along the different contact time. The biosorption rate of JES, RES and PES toward Cr(VI) removal was higher at the initial period of the biosorption process and then gradually decreased, reached almost constant when equilibrium was attained (Figure not shown). The equilibrium was established for JES, RES and PES almost near to 80, 100 and 60 min for all initial Cr(VI) concentrations. The results of the contact time of JES, RES and PES for different initial Cr(VI) concentration were further used successfully for assessment over the kinetics of the biosorption process.

Effect of temperature

The influence of temperature from 303 to 323 K was examined on the biosorption of 20 mg/L initial Cr(VI) concentration at pH 2.0 using JES, RES and PES, respectively (Fig. 4e). The experimental results indicated that the biosorption capacity of JES, RES and PES increased from 9.96 to 9.98, 8.15 to 9.83 and 8.94 to 9.98 mg/g, respectively, and the percentage Cr(VI) removal using JES, RES and PES increased from 99.66 to 99.88, 81.57 to 98.31 and 89.43 to 99.88%, respectively, with an increase in temperature from 303 to 323 K. The results reveals that the temperature has more influence on the Cr(VI) biosorption using RES and PES, than JES biosorbent. The increase in Cr(VI) biosorption with an increase in temperature may be due to the raised number of the biosorption sites on the biosorbents, increased kinetic energy of the Cr(VI) ions (Gholamreza and Behnam 2010), and this may lead to more biosorption on the surfaces of the biosorbents.

Biosorption isotherm study

The amount of Cr(VI) biosorbed onto JES, RES and PES at their respective equilibrium time for different initial Cr(VI) concentrations was determined at pH 2.0. The biosorption isotherm studies were analyzed using two parameter biosorption isotherm models like Langmuir, Freundlich, Dubinin–Radushkevich, Halsey, Flory–Huggins, Temkin and Jovanovic, respectively. Based on the coefficient of determination (R^2) and mean squared errors (MSE), the better fitted isotherm model explaining the biosorption of Cr(VI) from aqueous solutions by JES, RES and PES was evaluated. An analysis over the biosorption isotherm models was carried out, and the values of each isotherm model parameter along with the R^2 and MSE are presented in Table 3.

The isotherm data are linearized using the Langmuir isotherm model and are plotted between C_e/q_e versus C_e. The plots of JES, RES and PES were found almost linear, which indicates that the equilibrium data fitted well to the Langmuir model. The values of Q_0 and K_L calculated using the Langmuir plot are mentioned in Table 3. The maximum biosorption capacity obtained using Langmuir isotherm model for JES, RES and PES is 28.57, 19.60 and 27.77 mg/g, respectively. The Langmuir equilibrium constant was found as 1.2962 (JES), 0.1140 (RES) and 0.0965 (PES) L/mg. The high value of R^2 0.996 (JES), 0.984 (RES), 0.947 (PES) and low value of *MSE* 0.0022 (JES), 0.0024 (RES) and 0.0283 (PES) represent better agreement between the biosorption equilibrium data and Langmuir isotherm

Table 3 Comparison of the isotherms constants and coefficient of determination for the biosorption of hexavalent chromium onto JES, RES and PES

Isotherm models	Model constants	Values		
		JES	RES	PES
Langmuir	Q_0 (mg/g)	28.57	19.60	27.77
	K_L (L/mg)	1.2962	0.1140	0.0965
	R^2	0.996	0.984	0.947
	MSE	0.0022	0.0024	0.0283
	R_L			
	20	0.0371	0.3048	0.3412
	40	0.0189	0.1798	0.2057
	60	0.0126	0.1275	0.1472
	80	0.0095	0.0988	0.1146
	100	0.0076	0.0806	0.0938
Freundlich	K_f (mg/g)	17.57	5.63	6.68
	n	7.4626	3.6900	3.2362
	R^2	0.832	0.995	0.953
	MSE	0.4792	0.0015	0.0102
Dubinin–Radushkevich	Q_m (mg/g)	26.18	15.07	18.80
	K (mol^2/J^2)	2×10^{-8}	2×10^{-6}	8×10^{-7}
	E (kJ/mol)	5.0	0.5	0.8
	R^2	0.981	0.789	0.690
	MSE	0.0314	0.0838	0.2555
Halsey	K_H	5.10×10^{-8}	1.68×10^{-3}	2.13×10^{-3}
	n_H	−7.4626	−3.6900	−3.2362
	R^2	0.832	0.995	0.953
	MSE	0.5547	0.0015	0.0724
Flory–Huggins	K_{FH}	0.1034	0.0684	0.0778
	n_{FH}	−0.365	−1.838	−1.283
	R^2	0.919	0.940	0.904
	MSE	0.0442	0.0058	0.0489
Temkin	A_T (L/g)	2626.47	2.7639	2.4381
	b_T (kJ/mol)	1.0422	0.7366	0.5501
	R^2	0.904	0.968	0.886
	MSE	0.0428	0.0123	0.0796
Jovanovic	q_{mj} (mg/g)	15.55	8.83	9.54
	K_j (L/g)	−0.007	−0.005	−0.008
	R^2	0.532	0.899	0.937
	MSE	0.3588	0.0633	0.0221

parameters. The better fit of experimental data on the Langmuir biosorption isotherm model confirms the biosorption with monolayer coverage of Cr(VI) onto JES, RES and PES, respectively. The values (Table 3) of Langmuir separation factor (R_L) results revealed that the obtained values remained between 0.0371–0.0076 (JES), 0.3048–0.0806 (RES) and 0.3412–0.0938 (PES) for initial Cr(VI) concentration from 20 to 100 mg/L, suggested that the biosorption of Cr(VI) using JES, RES and PES was consistent with the requirement for a favorable biosorption process. Though the Langmuir biosorption isotherm model showed better agreement with the equilibrium data, in order to check the feasibility of other isotherms, the results are further analyzed with Freundlich, Dubinin–Radushkevich, Halsey, Flory–Huggins, Temkin and Jovanovic isotherm models considered in the present study.

The Freundlich isotherm model parameter was obtained from the linear plot of $\log(q_e)$ versus $\log(C_e)$. The values of R^2 and MSE of RES and PES are quite comparable to the R^2 and MSE value obtained for the Langmuir isotherm model. The value of low R^2 and high MSE in case of JES indicated that equilibrium data were not fitted well with the

Freundlich isotherm model. The biosorption intensity values of JES, RES and PES are 7.4626, 3.6900 and 3.2362 (Table 3), which are > 1.0 and represent the favorable Cr(VI) biosorption process. The parameters of Dubinin–Radushkevich isotherm model were calculated from the slope and the intercept of the linear plot of $\ln(q_e)$ versus ε^2 and the results are given in Table 3. The biosorption capacity predicted according to this model was 26.18, 15.07 and 18.80 mg/g for JES, RES and PES, respectively. The obtained biosorption capacity values were found lower than the Langmuir model predicted biosorption capacity, which may be because of the different assumptions consideration. The R^2 value of 0.981 (JES), 0.789 (RES) and 0.690 (PES) was found lower than the Langmuir and Freundlich isotherm model, except R^2 value of JES found higher than Freundlich isotherm model. High *MSE* value was observed for RES and PES. The Halsey biosorption isotherm parameters, K_H and n_H (Table 3), were obtained from the plot of $\ln(q_e)$ versus $\ln(C_e)$. The fitting of the experimental data to Halsey isotherm model demonstrates to the heteroporous nature of the biosorbent. The analysis of R^2 and MSE value of JES, RES and PES indicated that the Halsey biosorption isotherm model showed better agreement with experimental data in the biosorption of Cr(VI) using RES and PES in comparison with JES.

The values of Flory–Huggins model isotherm parameters, n_{FH} and K_{FH}, are calculated from the linear plot of $\log(Q/C_0)$ versus $\log(1-Q)$. The low values of K_{FH} and negative values of n_{FH} (Table 3) of JES, RES and PES indicated that the Flory–Huggins isotherm model cannot be used to illustrate the equilibrium data of Cr(VI) removal. Further, the values of R^2, 0.919 (JES), 0.940 (RES) and 0.904 (PES) were found less and higher MSE value represented the less applicability of this model. The Temkin isotherm parameters were determined from the linear plot of q_e versus $\ln(C_e)$. Lower values of b_T (Table 3), 1.0422 (JES), 0.7366 (RES) and 0.5501 kJ/mol (PES) specified that there is a weak ionic interaction between Cr(VI) and biosorbent. The R^2 value of 0.904 (JES), 0.968 (RES), 0.886 (PES) was found lower and *MSE* value of 0.0428 (JES), 0.0123 (RES), 0.0796 (PES) found higher than the Langmuir isotherm model. The parameters of the Jovanovic isotherm model were obtained from the linear plot of $\log(q_e)$ versus C_e. According to this model, the biosorption capacities were calculated as 15.55, 8.83 and 9.54 mg/g (Table 3) for JES, RES and PES, respectively, The maximum biosorption capacities of all the three biosorbents toward Cr(VI) removal based on the Jovanovic model were observed lower than Langmuir maximum biosorption monolayer capacities. The low R^2 and high *MSE* value for JES represent the least applicability of this model to the biosorption equilibrium data of JES.

Table 4 The Kinetics constants for the biosorption of Cr(VI) by JES, RES and PES

C_0 (mg/L)	Pseudo-first-order			Pseudo-second-order			Intraparticle diffusion		
	k_1 (1/min)	q_e (mg/g)	R^2	k_2 (g/mg min)	q_e (mg/g)	R^2	k_{id} (mg/g $\min^{1/2}$)	I (mg/g)	R^2
JES									
20	0.0529	4.6451	0.863	0.0334	10.3092	0.999	0.194	8.084	0.901
40	0.0529	12.1338	0.946	0.0107	20.8333	0.999	0.613	14.02	0.859
60	0.0506	17.3780	0.951	0.0058	26.3157	0.999	0.932	15.31	0.895
80	0.0368	25.0610	0.866	0.0040	28.5714	0.997	1.152	14.93	0.950
100	0.0322	18.0301	0.876	0.0031	31.2500	0.996	1.355	14.95	0.946
RES									
20	0.0368	7.3620	0.953	0.0062	9.4339	0.991	0.521	2.903	0.959
40	0.0253	10.6169	0.965	0.0028	14.2587	0.992	0.937	2.110	0.984
60	0.0345	14.2560	0.947	0.0023	17.2413	0.991	1.118	2.797	0.968
80	0.0322	15.3461	0.961	0.0022	19.6078	0.993	1.227	3.923	0.971
100	0.0299	14.2889	0.946	0.0028	20.4081	0.992	1.125	6.256	0.982
PES									
20	0.0299	8.2035	0.946	0.0052	10.5263	0.994	0.746	1.724	0.872
40	0.0368	11.6144	0.921	0.0038	15.3846	0.992	0.928	4.156	0.873
60	0.0506	17.9060	0.937	0.0037	20.4081	0.992	1.159	6.879	0.838
80	0.0437	19.4984	0.961	0.0025	24.3902	0.993	1.390	7.938	0.855
100	0.0460	22.7509	0.968	0.0027	27.777	0.994	1.605	9.224	0.848

Biosorption kinetic study

The constants of pseudo-first-order, pseudo-second-order and intraparticle diffusion kinetic models were obtained from the Eqs. (11), (12) and (13), respectively. The results of the kinetic constants and the coefficient of determination values for the removal of Cr(VI) by JES, RES and PES are shown in Table 4. The coefficient of determination of pseudo-first-order kinetic model was in the range of 0.863–0.951 (JES), 0.946–0.965 (RES) and 0.921–0.968 (PES), while for the pseudo-second-order kinetic model the R^2 values were in the range of 0.999–0.996 (JES), 0.993–0.991 (RES) and 0.994–0.992 (PES) for all the Cr(VI) concentrations. Further, the results of intraparticle diffusion kinetic model (Table 4) showed that the coefficient of determination ranged from 0.859 to 0.950 (JES), 0.959 to 0.984 (RES) and 0.838 to 0.873 (PES). On the basis of these results, it was observed that the biosorption of Cr(VI) onto JES, RES and PES was well described by the pseudo-second-order kinetic model and biosorption experimental data were not fitted well with the pseudo-first-order and intraparticle diffusion kinetic models. The suitability of the pseudo-second-order kinetic model reveals that the biosorption of Cr(VI) onto JES, RES and PES was governed by chemisorption mechanism which was associated with the valence forces participation through electrons sharing (Yunhai et al. 2017) between biosorbents and Cr(VI) ions.

Thermodynamic studies

The values of Gibbs free energy ($\Delta G°$) were calculated using Eq. (14), and the enthalpy change ($\Delta H°$) and entropy change ($\Delta S°$) values were obtained from the slope and intercept of the plot $\ln(K_c)$ versus $1/T$. The calculated thermodynamic parameters are summarized in Table 5. It was noticed from Table 5, for all the temperature, the values of Gibbs free energy were negative for JES, RES and PES represented the spontaneous nature of Cr(VI) biosorption process. The positive value of entropy change of 0.188 (JES), 0.349 (RES) and 0.635 kJ/mol K (PES) indicated the increased randomness at the biosorbent–aqueous solution boundary during the binding of the Cr(VI) ions onto the biosorbents active sites. Furthermore, the positive value of enthalpy change of 44.64 (JES), 104.43 (RES) and 189.05 kJ/mol K (PES) showed the endothermic nature of the biosorption process and increasing temperature favors the higher Cr(VI) removal. The higher enthalpy change value exemplified that the Cr(VI) biosorption using JES, RES and PES was based on chemisorption mechanism (Liang et al. 2013).

Table 5 The thermodynamic parameters for the biosorption of Cr(VI) onto JES, RES and PES at different temperatures

T (K)	JES				RES				PES			
	$\ln(K_c)$	$\Delta G°$ (kJ/mol)	$\Delta H°$ (kJ/mol)	$\Delta S°$ (kJ/mol K)	$\ln(K_c)$	$\Delta G°$ (kJ/mol)	$\Delta H°$ (kJ/mol)	$\Delta S°$ (kJ/mol K)	$\ln(K_c)$	$\Delta G°$ (kJ/mol)	$\Delta H°$ (kJ/mol)	$\Delta S°$ (kJ/mol K)
303	4.99	−12.58	44.64	0.188	0.79	−2.00	104.43	0.349	1.44	−3.63	189.05	0.635
313	5.40	−14.05			1.58	−4.11			3.51	−9.15		
323	6.09	−16.37			3.37	−9.05			6.09	−16.37		

Regeneration studies

The biosorbents regeneration was performed on the basis of general assumption that the regenerated biosorbents may promote in a cost-effective metal removal process. Desorption of Cr(VI)-loaded biosorbents with biosorption capacity of 9.96 mg/g (JES), 8.15 mg/g (RES) and 8.94 mg/g (PES) was performed separately with the desorbing agent of 0.1 M NaOH solution. In order to utilize the Cr(VI)-desorbed bisorbents for reusability, after the desorption process the JES, RES and PES were washed gently with distilled water to remove NaOH, oven dried further without any loss of biosorbents. The regenerated biosorbents was examined for a biosorption cycle using the same experimental condition of the batch biosorption study carried out. The biosorption capacity of the recycled JES, RES and PES was found as 9.79 mg/g, 7.68 and 8.86 mg/g. The results did not show noticeable change in the biosorption capacity for all the three biosorbents during a repeated biosorption investigation. Therefore, JES, RES and PES may be repeatedly used in Cr(VI) biosorption studies with their consistent initial biosorption capacity without much significant losses. The fully exhausted biosorbent can be employed as post-sorbent material in agricultural soil to improve nutritional qualities, to attain increased crop production yields and for enhanced water-holding capacity, and finally the biomass may undergo easy degradation. However, prior to the application of post-sorbent in the form of fertilizer or as soil conditioner, the determination over the levels of potential toxic elements in the post-sorbent biomass is highly indispensible (Reddy et al. 2017).

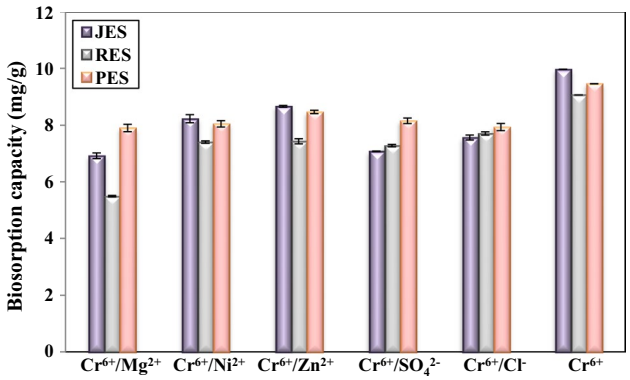

Fig. 5 Effect of coexisting ions on the biosorption capacity of JES, RES and PES toward Cr(VI) removal

Effect of coexisting ions on Cr(VI) biosorption capacity

Industrial effluent may contain a large number of cations and anions which may have competitive effect on the biosorption of Cr(VI). Hence, in the present study effect of commonly occurring ions like Mg^{2+}, Ni^{2+}, Zn^{2+}, SO_4^{2-}, Cl^- on the biosorption of Cr(VI) using JES, RES and PES was investigated. The initial concentration of all ions was kept constant at 20 mg/L along with 20 mg/L initial Cr(VI) concentration. Figure 5 illustrates the biosorption capacity of PES, JES and RES toward Cr(VI) removal in binary component system and compared to samples without coexisting ions. The results indicated that the presence of coexisting ions caused slight decrease in the biosorption capacity of Cr(VI) by JES and RES, this mechanism may be due to competitive effect. In case of PES biosorbent, the biosorption capacity was not affected by the presence of coexisting ions and the removal potential may be attributed to the phenomenon of ions binding without competition because of the presence of more biosorption site on the biosorbent.

Mechanism of Cr(VI) biosorption

The biomass of JES, RES and PES composed of complex structure with various functional groups, and the biosorption mechanisms associated with the interactions between the functional groups present on the biosorbent and Cr(VI) ions in the aqueous solutions. The complex structure of JES, RES and PES involvement in the biosorption process is connected with mechanism aspects of either physisorption or chemisorptions. The results of biosorption characterization study performed, FT-IR showed significant level of functional group involvement in the Cr(VI) removal process. The major peak shift regions after interaction with Cr(VI) are attributed to the functional groups such as OH stretching vibrations, N–H stretching, aromatic compounds bending vibrations (JES), OH stretching vibrations, –NH stretching, COO– group, bending vibrations of aromatic compounds (RES) and C=O stretching, N–H stretching, bending vibrations of aromatic compounds (PES). Moreover, the results obtained from the model analysis of better fitted isotherms (Langmuir) and kinetic studies (pseudo-second-order) revealed that the chemisorption mechanism as predominant in the removal of Cr(VI) from aqueous solution using JES, RES and PES, respectively.

Table 6 The comparison of biosorption capacities of JES, RES and PES with other biosorbents for the removal of Cr(VI) from aqueous solutions

Biosorbent	Initial pH	Biosorption capacities (mg/g)	References
Sal sawdust	3.5	9.55	Saroj et al. (2006)
Rice husk	2.0	8.50	Manjeet et al. (2009)
Dried pineapple leaves	2.0	18.77	Josiane et al. (2011)
Erythrina Variegata Orientalis leaf	3.0	1.92	Gannavarapu et al. (2012)
Ficus carica	3.0	19.68	Gupta et al. (2013)
Peanut shell	2.0	13.89	AL-Othman et al. (2012)
Ficus auriculata leaves	2.0	13.33	Rangabhashiyam et al. (2015)
Litchi peel	1.0–4.0	7.05	Yunhong et al. (2017)
Enteromorpha sp.	2.0	5.34	Rangabhashiyam et al. (2016)
Soy hull	1.5	7.28	Patricia et al. (2016)
Acacia albida Barks	2.0	2.98	Gebrehawaria et al. (2015)
JES	2.0	28.57	Present study
RES	2.0	19.60	Present study
PES	2.0	27.77	Present study
Swietenia mahagoni shells	2.0	37.03	Rangabhashiyam and Selvaraju (2015c)
Sterculia guttata shell	2.0	45.45	Rangabhashiyam and Selvaraju (2015d)
Pterospermum acerifolium shells	2.0	76.92	Rangabhashiyam and Balasubramanian (2018b)

Conclusion

Biosorbents from biodiesel extracted seeds of *Jatropha* sp., *Ricinus* sp. and *Pongamia* sp. were prepared and used successfully for the biosorption of Cr(VI) from aqueous solutions. Biosorption equilibrium experiments were found highly dependent on solution pH, biosorbent size, biosorbent dosage, initial Cr(VI) concentration and contact time. Among the biosorbents considered in the present study, RES showed lower Cr(VI) percentage removal (81.57%) compared to JES (99.66%) and PES (89.40%). The optimum solution pH was found as 2.0 for the removal of Cr(VI) by the biosorbents. The biosorption equilibrium data were satisfactorily explained by Langmuir isotherm model with the maximum biosorption capacity of 28.57, 19.60 and 27.77 mg/g for JES, RES and PES, respectively. Table 6 summarizes the comparison of the maximum biosorption capacities of various biosorbents together with the present study explored biosorbents for the removal of Cr(VI) from aqueous solutions. The rate of Cr(VI) removal using the biosorbents followed pseudo-second-order kinetic model with good coefficient of determination. The interactions between the Cr(VI) ions and the functional groups of the biosorbents confirmed the participation of the distinct functional groups toward the biosorption of Cr(VI) ions. Thermodynamic parameters for the removal of Cr(VI) using JES, RES and PES were estimated using equilibrium constants, obtained for the temperature range of 303–323 K. For all the three biosorbents, the negative values of ΔG° indicated the spontaneous nature of the Cr(VI) biosorption and the positive values of ΔH°, ΔS° represented endothermic and increased randomness during the Cr(VI) biosorption process. Experiments were conducted for the regeneration of biosorbents through 0.1 M NaOH desorbing agent and did not notice major change in the biosorption capacities of JES, RES and PES during a repeated biosorption process with an initial Cr(VI) concentration of 20 mg/L. The biosorption capacities of JES and RES toward Cr(VI) removal were slightly decreased, whereas the PES biosorbent uptake capacity remains unchanged in the presence of coexisting ions. The results of present investigations revealed that the waste biomass after biodiesel extraction from the seeds of *Jatropha* sp., *Ricinus* sp. and *Pongamia* sp. (JES, RES and PES) offered as the potential biosorbents for the removal of hexavalent chromium from aqueous solutions.

Acknowledgements The authors sincerely acknowledge the Science and Engineering Research Board, Department of Science and Technology, India, for the award of postdoctoral research Grant (PDF/2016/000284). The authors would like to thank the National Institute of Technology, Rourkela, for the research facility.

List of symbols

q_e	Equilibrium biosorption capacity (mg/g)
C_0	Initial Cr(VI) concentration (mg/L)
C_e	Cr(VI) concentration at equilibrium (mg/L)
V	Volume of the Cr(VI) solution (L)
m	Dry weight of the biosorbent (g)
Q_0	Biosorption capacity from Langmuir isotherm model (mg/g)
K_L	Langmuir equilibrium constant (L/mg)
R_L	Dimensionless equilibrium separation factor
K_f	Freundlich isotherm biosorption capacity (mg/g)
n	Biosorption intensity
Q_m	Dubinin–Radushkevich isotherm maximum biosorption capacity (mg/g)
K	Activity coefficient related to mean biosorption energy (mol^2/J^2)
ε	Polanyi potential of Dubinin–Radushkevich model
T	Temperature (K)
E	Mean biosorption energy (kJ/mol)
K_H	Halsey isotherm model constant
n_H	Halsey model exponent
K_{FH}	Flory–Huggins equilibrium constant
n_{FH}	Flory–Huggins model exponent
Q	Degree of surface coverage
b_T	Temkin constant (kJ/mol)
A_T	Equilibrium binding constant (L/g)
q_{mj}	Maximum multilayer biosorption capacity in Jovanovic model (mg/g)
K_j	Jovanovic isotherm constant (L/g)
k_1	Pseudo-first-order biosorption rate constant (1/min)
k_2	Pseudo-second-order biosorption rate constant (g/mg min)
k_{id}	Intraparticle diffusion model rate constant ($mg/g\ min^{1/2}$)
I	Intercept of Intraparticle diffusion model (mg/g)
$\Delta G°$	Gibbs free energy (kJ/mol)
$\Delta H°$	Enthalpy change (kJ/mol)
$\Delta S°$	Entropy change (kJ/mol K)
K_c	Distribution coefficient
R^2	Coefficient of determination

References

AL-Othman ZA, Ali R, Naushad M (2012) Hexavalent chromium removal from aqueous medium by activated carbon prepared from peanut shell: adsorption kinetics, equilibrium and thermodynamic studies. Chem Eng J 184:238–247

Anil KG, Rajkishore P, Sandip M (2012) Removal of Cr(VI) from aqueous solution by *Eichhornia crassipes* root biomass-derived activated carbon. Chem Eng J 185–186:71–81

Ayushi V, Shashi K, Surendra K (2017) Statistical modeling, equilibrium and kinetic studies of cadmium ions biosorption from aqueous solution using *S. filipendula*. J Environ Chem Eng 5:2290–2304

Dubinin MM, Radushkevich LV (1947) The equation of the characteristic curve of activated charcoal. Dokl Akad Nauk SSSR 55:327–329

Edidiong DA, Alastair DM (2016) Sorption of cadmium(II) ion from aqueous solution onto sweet potato (*Ipomoea batatas* L.) peel adsorbent: characterisation, kinetic and isotherm studies. J Environ Chem Eng 4:4207–4228

EPA (1990) Environmental pollution control alternatives EPA/625/5-90/25, EPA/625/4-89/023. Enviromental Protection Agency, Cincinaati

Freundlich H, Helle W (1939) On adsorption in solution. J Am Chem Soc 61:2228–2230

Gadd GM (2009) Biosorption: critical review of scientific rationale, environmental importance and significance for pollution treatment. J Chem Technol Biotechnol 84:13–28

Gannavarapu VVA, Bhagavatula PP, Nalluri CB, Paladugu V (2012) Biosorption of chromium onto *Erythrina Variegata Orientalis* leaf powder. Korean J Chem Eng 29:64–71

Gebrehawaria G, Hussen A, Rao VM (2015) Removal of hexavalent chromium from aqueous solutions using barks of *Acacia albida* and leaves of *Euclea schimperi*. Int J Environ Sci Technol 12:1569–1580

Gholamreza M, Behnam B (2010) Biosorption of chromium(VI) from industrial wastewater onto pistachio hull waste biomass. Chem Eng J 162:893–900

Gupta VK, Deepak P, Shilpi A, Shikha S (2013) Removal of Cr(VI) onto *Ficus carica* biosorbent from water. Environ Sci Pollut Res 20:2632–2644

Halsey G (1948) Physical adsorption on nonuniform surfaces. J Chem Phys 16:931–937

Ho YS, McKay G (1999) Pseudo-second order model for sorption processes. Process Biochem 34:451–465

Horsfall M, Spiff AI (2005) Equilibrium sorption study of Al^{3+}, Co^{2+} and Ag^{2+} in aqueous solutions by fluted pumpkin (*Telfairia occidentalis* HOOK) waste biomass. Acta Chim Slov 52:174–181

Hyder AHMG, Shamim AB, Nosa OE (2015) Adsorption isotherm and kinetic studies of hexavalent chromium removal from aqueous solution onto bone char. J Environ Chem Eng 3:1329–1336

Jinjuta K, Hyungseok N, Sergio C (2016) Capareda, Jatropha waste meal as an alternative energy source via pressurized pyrolysis: a study on temperature effects. Energy 113:631–642

Josiane P, Jungah K, Li PW, Gjergj D, Toyohisa F (2011) Sorption of Cr(VI) anions in aqueous solution using carbonized or dried pineapple leaves. Chem Eng J 172:906–913

Jovanovic DS (1969) Physical adsorption of gases I: isotherms for monolayer and multilayer adsorption. Colloid Polym Sci 235:1203–1214

Lagergren S (1898) About the theory of so-called adsorption of soluble substances. K Svenska Vetenskapsakad Handl 24:1–39

Langmuir I (1916) The constitution and fundamental properties of solids and liquids. J Am Chem Soc 38:2221–22295

Liang FB, Song YL, Huang CP, Zhang J, Chen BH (2013) Adsorption of hexavalent chromium on a lignin-based resin: equilibrium, thermodynamics, and kinetics. J Environ Chem Eng 1:1301–1308

Ma Y, Liu WJ, Zhang N, Li Y-S, Jiang H, Sheng G-P (2014) Polyethylenimine modified biochar adsorbent for hexavalent chromium removal from the aqueous solution. Bioresour Technol 169:403–408

Manjeet B, Umesh G, Diwan S, Garg VK (2009) Removal of Cr(VI) from aqueous solutions using pre-consumer processing agricultural waste: a case study of rice husk. J Hazard Mater 162:312–320

Mohankumar BV, Sharath BS, Somashekar D (2014) Solid-state fermentation of Jatropha seed cake for optimization of lipase, protease and detoxification of anti-nutrients in Jatropha seed cake using *Aspergillus versicolor* CJS-98. J Biosci Bioeng 117:208–214

Mojdeh O, Mohamed KA, Wan AWD, Saeid B (2009) Removal of hexavalent chromium-contaminated water and wastewater: a review. Water Air Soil Pollut 200:59–77

Namasivayam C, Sangeetha D (2006) Recycling of agricultural solid waste, coir pith: removal of anions, heavy metals, organics and dyes from water by adsorption onto $ZnCl_2$ activated coir pith carbon. J Hazard Mater 135:449–452

Oladoja NA, Ahmad AL, Adesina OA, Adelagun ROA (2012) Low-cost biogenic waste for phosphate capture from aqueous system. Chem Eng J 209:170–179

Panwar NL, Hemant YS, Bamniya BR (2010) CO_2 mitigation potential from biodiesel of castor seed oil in Indian context. Clean Technol Environ Policy 12:579–582

Patricia SB, Maria EB, Juan CG, Silvia IG, Ana MA, Luis FS, Sebastian EB (2016) Application of soy hull biomass in removal of Cr(VI) from contaminated waters. Kinetic, thermodynamic and continuous sorption studies. J Environ Chem Eng 4:516–526

Pehlivan E, Pehlivan E, Tutar Kahraman H (2012) Hexavalent chromium removal by Osage Orange. Food Chem 133:1478–1484

Radhakumari M, Andrew SB, Suresh KB, Satyavathi B (2016a) Bioethanol production from non-edible de-oiled *Pongamia pinnata* seed residue-optimization of acid hydrolysis followed by fermentation. Ind Crops Prod 94:490–497

Radhakumari M, Mohamed T, Esmaeil S, Suresh KB, Satyavathi B, Andrew SB (2016b) *Pongamia pinnata* seed residue-a low cost inedible resource for on-site/in-house lignocellulases and sustainable ethanol production. Renew Energy. https://doi.org/10.1016/j.renene.2016.10.082

Rahulkumar M, Tonmoy G, Hitesh S, Chetan P, Arup G, Sandhya M (2016) Non-isothermal pyrolysis of de-oiled microalgal biomass: kinetics and evolved gas analysis. Bioresour Technol 221:251–261

Rangabhashiyam S, Balasubramanian P (2018) Adsorption behaviors of hazardous methylene blue and hexavalent chromium on novel materials derived from *Pterospermum acerifolium* shells. J Mol Liq 254:433–445

Rangabhashiyam S, Selvaraju N (2015a) Evaluation of the biosorption potential of a novel *Caryota urens* inflorescence waste biomass for the removal of hexavalent chromium from aqueous solutions. J Taiwan Inst Chem Eng 47:59–70

Rangabhashiyam S, Selvaraju N (2015b) Efficacy of unmodified and chemically modified *Swietenia mahagoni* shells for the removal of hexavalent chromium from simulated wastewater. J Mol Liq 209:487–497

Rangabhashiyam S, Selvaraju N (2015c) Adsorptive remediation of hexavalent chromium from synthetic wastewater by a natural and $ZnCl_2$ activated *Sterculia guttata* shell. J Mol Liq 207:39–49

Rangabhashiyam S, Anu N, Giri Nandagopal MS, Selvaraju N (2014a) Relevance of isotherm models in biosorption of pollutants by agricultural byproducts. J Environ Chem Eng 2:398–414

Rangabhashiyam S, Suganya E, Selvaraju N (2014b) Significance of exploiting non-living biomaterials for the biosorption of wastewater pollutants. World J Microbiol Biotechnol 30:1669–1689

Rangabhashiyam S, Nakkeeran E, Anu N, Selvaraju N (2015) Biosorption potential of a novel powder, prepared from *Ficus auriculata* leaves, for sequestration of hexavalent chromium from aqueous solutions. Res Chem Intermed 41:8405–8424

Rangabhashiyam S, Suganya E, Lity AV, Selvaraju N (2016) Equilibrium and kinetics studies of hexavalent chromium biosorption on a novel green macroalgae *Enteromorpha* sp. Res Chem Intermed 42:1275–1294

Rangabhashiyam S, Lata Sujata, Balasubramanian P (2018) Biosorption characteristics of methylene blue and malachite green from simulated wastewater onto *Carica papaya* wood biosorbent. Surf Interfaces 10:197–215

Reddy DHK, Vijayaraghavan K, Kim JA, Yun YS (2017) Valorisation of post-sorption materials: opportunities, strategies, and challenges. Adv Colloid Interface Sci 242:35–58

Saroj SB, Surendra ND, Pradip R (2006) Hexavalent chromium removal from aqueous solution by adsorption on treated sawdust. Biochem Eng J 31:216–222

Shalini S, Agrawal SB, Mondal MK (2015) Biosorption isotherms and kinetics on removal of Cr(VI) using native and chemically modified *Lagerstroemia speciosa* bark. Ecol Eng 85:56–66

Somdutta S, Ujjaini S, Sourav M, Sudeshna S (2012) Transient behavior of a packed column of *Eichhornia crassipes* stem for the removal of hexavalent chromium. Desalination 297:48–58

Suresh G, Babu BV (2009) Utilization of waste product (tamarind seeds) for the removal of Cr(VI) from aqueous solutions: equilibrium, kinetics, and regeneration studies. J Environ Manag 90:3013–3022

Svitlana NY, Lucie C, Raphael S, Roger HCN, Yvonne LBC (2016) Ethyl biodiesel production from non-edible oils of *Balanites aegyptiaca*, *Azadirachta indica*, and *Jatropha curcas* seeds—laboratory scale development. Renew Energy 96:881–890

Swaroopa RD, Venu BB, Vaibhav VG (2016) Reactive extraction of castor seeds and storage stability characteristics of produced biodiesel. Process Saf Environ Prot 100:252–263

Tempkin MJ, Pyzhev V (1940) Kinetics of ammonia synthesis on promoted iron catalysts. A Physiochim URSS 12:217–222

Umesh KG, Kaur MP, Sud Dhiraj, Garg VK (2009) Removal of hexavalent chromium from aqueous solution by adsorption on treated sugarcane bagasse using response surface methodological approach. Desalination 249:475–479

Weber WJ, Morris JC (1962) Advances in water pollution research: removal of biologically resistant pollutants from waste waters by adsorption. In: Proceedings of international conference on water pollution symposium, vol 2. Pergamon Press, Oxford, pp 231–266

Wen S, Baoyu G, Tengge Z, Xing X, Xin H, Huan Y, Qinyan Y (2015) High-capacity adsorption of dissolved hexavalent chromium using amine-functionalized magnetic corn stalk composites. Bioresour Technol 190:550–557

Wu Y, Ming Z, Yang S, Fan Y, Feng P, Sha H, Cha L (2017) Adsorption of hexavalent chromium onto Bamboo Charcoal grafted by Cu^{2+}-*N*-aminopropylsilane complexes: optimization, kinetic, and isotherm studies. J Ind Eng Chem 46:222–233

Yi Y, Lv J, Liu Y, Wu G (2017) Synthesis and application of modified Litchi peel for removal of hexavalent chromium from aqueous solutions. J Mol Liq 225:28–33

Affiliations

S. Rangabhashiyam[1,3] · S. Sayantani[2] · P. Balasubramanian[1]

✉ S. Rangabhashiyam
rambhashiyam@gmail.com

[1] Department of Biotechnology and Medical Engineering, National Institute of Technology Rourkela, Rourkela, Odisha 769 008, India

[2] Department of Chemical Engineering, National Institute of Technology Rourkela, Rourkela, Odisha 769 008, India

[3] Department of Biotechnology, School of Chemical and Biotechnology, SASTRA University, Thanjavur, Tamilnadu 613401, India